HHS Public Access

Author manuscript

Circ Res. Author manuscript; available in PMC 2023 September 16.

Published in final edited form as:

Circ Res. ; : 101161CIRCRESAHA122321431. doi:10.1161/CIRCRESAHA.122.321431.

Fibroblast GSK-3α Promotes Fibrosis via RAF-MEK-ERK Pathway in the Injured Heart

Prachi Umbarkar, PhD[a], **Sultan Tousif, PhD**[a], **Anand P. Singh, PhD**[a], **Joshua C. Anderson, PhD**[b], **Qinkun Zhang, MD**[a], **Michelle D. Tallquist, PhD**[c], **James Woodgett, PhD**[d], **Hind Lal, PhD**[a]

[a]Division of Cardiovascular Disease, The University of Alabama at Birmingham, AL 35294-1913, USA

[b]Department of Radiation Oncology, The University of Alabama at Birmingham, AL 35294-1913, USA

[c]Center for Cardiovascular Research, University of Hawaii, Honolulu, USA

[d]Lunenfeld-Tanenbaum Research Institute, Mount Sinai Hospital, Toronto, ON, Canada

Abstract

Background—Heart failure (HF) is the leading cause of mortality, morbidity, and healthcare expenditures worldwide. Numerous studies have implicated Glycogen Synthase Kinase-3 (GSK-3) as a promising therapeutic target for cardiovascular diseases. GSK-3 isoforms appear to play overlapping, unique, and even opposing functions in the heart. Previously we have shown that of the two isoforms of GSK-3, cardiac fibroblast (CF) GSK-3β acts as a negative regulator of myocardial fibrosis in the ischemic heart. However, the role of CF-GSK-3α in the pathogenesis of cardiac diseases is completely unknown.

Methods: To define the role of CF-GSK-3α in myocardial fibrosis and HF, GSK-3α was deleted from fibroblasts or myofibroblasts with tamoxifen-inducible Tcf21- or Postn- promoter-driven Cre recombinase. Control and GSK-3α KO mice were subjected to cardiac injury and heart parameters were evaluated. The fibroblast kinome mapping was carried out to delineate molecular mechanism followed by *in vivo* and *in vitro* analysis.

Results: Fibroblast-specific GSK-3α deletion restricted fibrotic remodeling and preserved function of the injured heart. We observed reductions in cell migration, collagen gel contraction, α-SMA protein levels, and expression of ECM genes in TGFβ1-treated KO fibroblasts, indicating that GSK-3α is required for myofibroblast transformation. Surprisingly, GSK-3α deletion did not affect SMAD3 activation, suggesting the pro-fibrotic role of GSK-3α is SMAD3 independent. The molecular studies confirmed decreased ERK signaling in GSK-3α-KO CFs. Conversely, adenovirus-mediated expression of a constitutively active form of GSK-3α (Ad-GSK-3α^{S21A}) in

ADDRESS FOR CORRESPONDENCE Hind Lal, Ph.D., Associate Professor of Medicine, Division of Cardiovascular Disease, UAB | The University of Alabama at Birmingham, 1720 2nd Ave South, Birmingham, AL 35294-1913, Tel: 205.996.4219, Fax: 205.975.5104, hindlal@uabmc.edu.

Disclosures

The authors have no conflicting interests to disclose concerning this work.

fibroblasts increased ERK activation and expression of fibrogenic proteins. Importantly, this effect was abolished by ERK inhibition.

Conclusions: GSK-3α mediated MEK-ERK activation is a critical pro-fibrotic signaling circuit in the injured heart which operates independently of the canonical TGF-β1-SMAD3 pathway. Therefore, strategies to inhibit the GSK-3α-MEK-ERK signaling circuit could prevent adverse fibrosis in diseased hearts.

Graphical Abstract

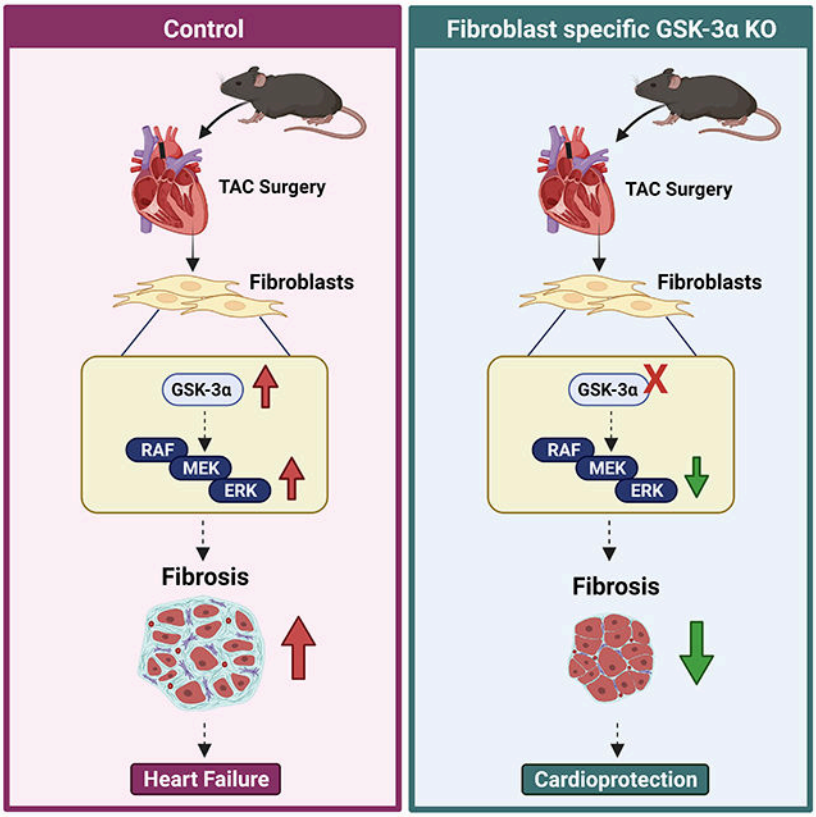

Keywords

GSK-3α; fibrosis; fibroblast; heart failure; ERK signaling

SUBJECT CODES

Mechanisms; Basic Science Research; Cell Signaling/Signal Transduction

Introduction

Myocardial fibrosis contributes significantly to heart failure (HF) progression.[1-3] However, there is no specific therapy to combat myocardial fibrosis. The cardiac fibroblasts (CF), one of the major cell types in the heart [4], are key contributors to the development of fibrosis.[5] Until recently, the role of CF in cardiac pathophysiology remained auxiliary to

cardiomyocytes, in part because animal models that permit CF-specific gene targeting were unavailable. Thus, most of the literature regarding fibroblast biology has largely relied on experimental outcomes emerging from *in vitro* culture systems and mouse models in which the target gene is deleted in cardiomyocytes or globally. To overcome this limitation, the scientific community has developed fibroblast-specific genetic mouse models.[6] Among the recently generated FB-specific genetic models, Tcf21^{MCM} and Postn^{MCM} mice lines are well characterized and suited for the effective manipulation of a target gene in the tissue-resident fibroblasts and myofibroblasts, respectively.[7-13]

Myocardial fibrosis is characterized by a disproportionate accumulation of extracellular matrix (ECM) components. In an injured heart, CFs undergo a phenotypic switch from a quiescent to an activated state. These activated CFs or myofibroblasts are considered to be the principal producers of ECM under pathological conditions.[5] Among various pro-fibrotic factors, TGFβ1 is best characterized for its role in fibroblast activation and has been implicated in promoting fibrosis in various cardiac diseases. In canonical TGFβ signaling, the binding of TGFβ to its receptors leads to the activation of receptor-associated SMADs. These activated SMADs form a heteromeric complex with co-SMAD, i.e., SMAD4, which then translocates into the nucleus and regulates the transcription of target genes. In addition to this canonical signaling, TGFβ can modulate the signaling of mitogen-activated protein kinases (MAPKs), phosphoinositide-3-kinase (PI3K), Ras Homolog Family Member A (RhoA), protein phosphatase 2A (PP2A), nuclear factor-κB (NF-kB), and TGF-β-activated kinase 1 (TAK1).[14] Our lab has demonstrated the CF-specific deletion of Glycogen Synthase Kinase-3β (GSK-3β) causes hyperactivation of SMAD-3, which results in excessive fibrosis and cardiac dysfunction post-MI.[15] Also, fibroblast-specific genetic manipulation revealed that MAPK p38α acts as a nodal point where mechanical and paracrine signals converge to initiate a fibrotic response in the mouse heart.[10] A recent study has shown that TGF β1 increases IL-11 expression in fibroblasts which, in turn, regulates the translation of fibrogenic proteins via a non-canonical, ERK-dependent pathway.[16] Together, these studies indicate that multiple distinct pathways cooperate with classical TGF β signaling in fibroblasts to mediate fibrotic responses in the diseased or damaged heart.

The GSK-3 family is comprised of two highly conserved isoforms, GSK-3α and GSK-3β. The roles of GSK-3 isoforms in cardiomyocyte biology and cardiac disease have been extensively studied.[15, 17-23] Our lab has discovered that CF-GSK-3β acts as a negative regulator of myocardial fibrosis in the ischemic heart.[15] However, the role of CF-GSK-3α in the pathogenesis of HF is entirely unknown. We found that CF-GSK-3α activity increases as an early response to pressure overload (Figure S1). In the present study, we employed Tcf21^{MCM} and Postn^{MCM} models to delete GSK-3α specifically from resident cardiac fibroblasts and myofibroblasts. We report that CF-specific deletion of GSK-3α prevents pressure overload-induced adverse fibrotic remodeling and cardiac dysfunction. Mechanistically, we demonstrate that GSK-3α exerts its pro-fibrotic effect via the RAF-MEK-ERK signaling network and is independent of classical canonical TGF-β1/SMAD3 signaling.

Methods

Data Availability

The data that support the findings of this study are available from the corresponding author upon reasonable request.

Mice

Resident fibroblast-specific deletion of GSK-3α (GSK-3α^{FKO}) was achieved by crossing GSK-3α $^{fl/fl}$ mice [24, 25] with Tcf21^{MCM} mice[12, 26]. To generate myofibroblast-specific GSK-3α KO (GSK-3α^{MFKO}), GSK-3α $^{fl/fl}$ mice were crossed with Periostin-MCM mice (Postn^{MCM}; Jackson laboratories, stock #029645).[11] The GSK-3α $^{fl/fl}$/Cre$^{+/-}$/TAM mice were denoted as fibroblast knockouts (GSK-3α^{FKO} or GSK-3α^{MFKO}), whereas littermates GSK-3α $^{fl/fl}$/Cre$^{-/-}$/TAM represented as controls (CTL). A cohort of animals of both sexes was recruited to investigate the sex-specific role of FB-GSK-3α on cardiac function. We did not observe sex-specific differences in our models (Figure S2). No animals were excluded from the analysis. The Institutional Animal Care and Use Committee of the University of Alabama at Birmingham approved all animal procedures and treatments used in this study (protocol # IACUC-21701).

Statistical analysis

Analyses were performed using GraphPad Prism (version 9.0.0). The Shapiro-Wilk test was used to determine the normality of data. Data following normal distribution were then analyzed with an unpaired, 2-tailed Student *t*-test (2 groups). For multiple group comparisons, 1-way ANOVA (for 1 variable) or 2-way ANOVA (for 2 variables) was conducted followed by Tukey post hoc analysis. For non-normally distributed data or when N<6, unpaired 2-tailed Mann-Whitney test (for 2 groups) or Kruskal-Wallis test (for 3 or more groups) was performed, followed by Dunn post hoc analysis. A p-value of < 0.05 was considered statistically significant.

Detailed descriptions of experimental methods are presented in Supplemental Material.

Results

Deletion of GSK-3α in residential FBs prevents adverse cardiac remodeling and maintains cardiac function.

Among the two isoforms of the GSK-3 family of kinases, the role of GSK-3β in fibrotic signaling is well known. However, there is no literature on the role of GSK-3α in fibrosis biology.[15, 17-21] We found that CF-GSK-3α activity increases as an early response to pressure overload (Figure S1). To evaluate the role of cardiac resident fibroblast GSK-3α in injury-induced cardiac remodeling, we generated a mouse model in which GSK-3α was conditionally deleted in resident fibroblast using tamoxifen (TAM)-inducible Tcf21 promoter-driven MerCreMer transgene (Tcf21-MCM). We crossed Tcf21^{MCM} mice with GSK-3α$^{fl/fl}$ mice to obtain GSK-3α$^{fl/fl}$Tcf21^{MCM} mice. GSK-3α$^{fl/fl}$/MCM$^{+/-}$/TAM mice were denoted as knockout (GSK-3α^{FKO}), whereas littermates GSK-3α $^{fl/fl}$/MCM$^{-/-}$/TAM represented controls (CTL). Tamoxifen (TAM) chow diet protocol was employed to induce

the FB-specific expression of Cre recombinase, as previously reported.[8] To confirm the CF-specific deletion of GSK-3α, fibroblasts were isolated from the heart of experimental animals and proteins were extracted. Western blot analysis confirmed that TAM treatment led to a significant reduction of GSK-3α protein in the CFs from GSK-3α^{FKO} mice compared with littermate controls (Figure 1A-1B).

After 2 weeks of TAM treatment, mice were subjected to TAC surgery. To assess cardiac function, we performed serial M-mode echocardiography. In the CTL-TAC group, LVEF and LVFS declined from 4 weeks post-surgery, indicating systolic dysfunction (Figure 1C-1D). These changes were associated with the development of structural remodeling as reflected by a significant increase in LVIDs, in the CTL-TAC group (Figure 1E-1F). Interestingly, all these parameters were essentially normalized in GSK-3α^{FKO}. To verify the effects of CF-specific GSK-3α deletion on adverse cardiac remodeling, we performed morphometrics and histological studies at 8 weeks post-TAC. We measured HW/TL ratio and cardiomyocyte cross-sectional area (CSA). Both these parameters were elevated in the CTL-TAC group revealing hypertrophic remodeling (Figure 2A-2B). For assessment of cardiac fibrosis, Masson's Trichrome staining was used, and excessive collagen deposition was detected in CTL-TAC hearts (Figure 2C-2D). Since activated fibroblasts or myofibroblasts are the key contributors to fibrosis and are characterized by α-SMA expression, we measured α-SMA^{+ve} non-vascular cells. Immunofluorescence studies confirmed increase in α-SMA^{+ve} non-vascular cells in the CTL-TAC heart as compared to the CTL-SHAM group (Figure 2E-2F). All these characteristics of pathological cardiac remodeling were alleviated in GSK-3α^{FKO} mice. Additionally, we compared expression levels of key genes related to cardiac hypertrophy (ANP and BNP) and fibrosis (COL1A1 and COL3A1). These molecular markers were significantly augmented in the CTL-TAC group but were normalized in GSK-3α^{FKO} mice (Figure 2G-2J). Taken together, these findings confirmed that deletion of GSK-3α from resident FBs before injury insult resulted in improved cardiac function and prevented adverse cardiac remodeling post-TAC. To confirm whether fibrosis is the primary factor contributing to cardiac phenotype and not the mere secondary effect of adverse remodeling, we assessed myocardial fibrosis and cardiomyocyte hypertrophy at 4 weeks post-TAC, a time point that preceded major functional differences between genotypes. Indeed, fibroblast-specific deletion of GSK-3α significantly reduced cardiac fibrosis. Importantly, cardiomyocyte hypertrophy remained comparable between the groups (Figure S3). These findings suggest that fibrosis is central to the protection conferred by fibroblast-specific GSK-3α deletion

Deletion of GSK-3α in myofibroblasts protects the heart from injury-induced adverse cardiac remodeling and dysfunction.

Cardiac injury triggers the activation of fibroblasts by a process called myofibroblast transformation. Myofibroblasts play a key role in the healing phase of injury. However, persistent survival of these cells even after injury resolution leads to pathological fibrotic remodeling and cardiac dysfunction.[5] To define the role of GSK-3α in myofibroblast function, we deleted GSK-3α specifically in myofibroblasts using tamoxifen (TAM)-inducible periostin promoter-driven MerCreMer transgene (Postn^{MCM}). We crossed Postn^{MCM} mice with GSK-3α$^{fl/fl}$ mice to obtain GSK-3α$^{fl/fl}$Postn^{MCM} mice. GSK-3α$^{fl/fl}$/

MCM$^{+/-}$/TAM mice were designated as conditional knockout (GSK-3α^{MFKO}), whereas littermates GSK-3α $^{fl/fl}$/MCM$^{-/-}$/TAM represented wild type controls (CTL). Tamoxifen (TAM) chow diet protocol was employed to induce the FB-specific expression of Cre recombinase, as previously reported.[8] To confirm the CF-specific deletion of GSK-3α, fibroblasts were isolated from the heart of experimental animals at 4 weeks post-injury, and proteins were subjected to Western blot analysis which confirmed that TAM treatment caused a significant reduction of GSK-3α protein in the CFs from GSK-3α^{MFKO} mice compared with littermate controls (Figure 3A-3B).

After 1 week of TAM treatment, mice were subjected to TAC surgery. We assessed cardiac function by serial echocardiography. The CTL-TAC group showed lower LVEF and LVFS as compared to CTL-SHAM, confirming the development of cardiac dysfunction. Moreover, LVIDs were significantly increased in CTL-TAC groups, indicating the development of adverse cardiac remodeling. All these injury-induced adverse effects were remarkably prevented by myofibroblast-specific GSK-3α deletion (Figure 3C-3F).

To further examine the cardioprotective effects of myofibroblast-specific GSK-3α deletion on cardiac remodeling, we harvested the hearts at 8 weeks post-TAC for morphometrics and histological studies. The CTL-TAC group showed a significant increase in HW/TL and CSA compared with the CTL-SHAM group, indicative of cardiac hypertrophy. These parameters were comparatively lowered in hearts where myofibroblast-specific GSK-3α deletion had occurred (Figure 4A-4B). Masson's Trichrome staining revealed excessive collagen deposition in CTL-TAC groups. Also, the number of α-SMA^{+ve} non-vascular cells was higher in the CTL-TAC group, confirming the development of adverse cardiac fibrosis in these animals (Figure 4C-4F). Notably, loss of GSK-3α from myofibroblasts exerted a major impact on cardiac fibrosis by normalizing it to that of the CTL-SHAM group. Next, we analyzed the expression of signature genes related to cardiac hypertrophy (ANP and BNP) and cardiac fibrosis (COL1A1, COL3A1) by the qPCR method. As expected, there was a significant increase in levels of these molecular markers in the CTL-TAC group, and deletion of GSK-3α from myofibroblasts caused retention of normal levels (Figure 4G-4J). Taken together, these findings suggest that deletion of GSK-3α post-injury affects myofibroblast function and delays injury-induced pathological remodeling.

CF-GSK-3α promotes Fibroblast to Myofibroblast Transformation

To define the role of GSK-3α in fibrotic remodeling, we examined the effect of GSK-3α deletion on myofibroblast transformation, a key event in fibrosis. Myofibroblasts are hyper-migratory and exhibit hyper-contractile nature. To validate their phenotype, we performed cell migration and collagen gel contraction assays, which are based on these key characteristics. To induce myofibroblast transformation, we treated WT and GSK-3α KO mouse embryonic fibroblasts (MEFs) with TGF-β1 (10 ng/mL, 48h). We observed a reduction in α-SMA protein levels, cell migration and collagen gel contraction in TGF-β1 treated GSK-3α KO MEF (Figure 5A-5E). Additionally, ECM gene expression (COL1A1, Fibronectin-1) was downregulated in KO cells (Figure 5F-5G). These findings are consistent with a requirement for GSK-3α in TGF-β1-induced myofibroblast transformation and fibrotic response.

CF-GSK-3α mediates pro-fibrotic effects independent of canonical TGF-β1-SMAD3 signaling

GSK-3 are well known for its regulatory role in glycogen synthesis and autophagy.[27, 28] However, we did not observe a significant alteration in levels of glycogen synthase in GSK-3α KO FBs indicating that FB glucose metabolism was unaltered and not contributing to GSK-3α mediated pro-fibrotic response (Figure S4). The role of autophagy in fibrosis is controversial hence future studies are needed to confirm the contribution of autophagy in FB-GSK-3α mediated pro-fibrotic response.

Historically, canonical TGF-β1-SMAD3 signaling has been at the center of the mechanistic basis of myocardial fibrosis. Furthermore, we have previously reported a critical role of CF-GSK-3β in TGF-β1-SMAD3 signaling; however, the role of GSK-3α in this well-known pro-fibrotic pathway is unidentified.[15] First, we confirmed whether GSK-3α deletion/overexpression has any effect on GSK-3β expression/activity in FBs. Our western blot analysis showed that GSK-3β expression/activity was not altered in GSK-3α KO or overexpressing FBs (Figure S5). To test whether GSK-3α may also modulate TGF-β1-SMAD3 signaling, we examined the effect of deleting this isoform on SMAD3 activation. WT and GSK-3α MEFs were treated with TGF-β1 (10ng/ml, 1h), and SMAD3 activation was confirmed by analyzing levels of SMAD3 phosphorylation and nuclear translocation. Surprisingly, TGF-β1-induced SMAD3 activation was comparable in both WT and GSK-3α KO MEF (Figure 6A-6B). We then isolated CFs from adult GSK-3α $^{fl/fl}$ mice and adenovirally transduced them with either LacZ (Ad-LacZ) as control or Cre recombinase (Ad-Cre) to delete GSK-3α, as described previously.[15] Western blot analysis confirmed that Ad-Cre transduction led to an 80% reduction in GSK-3α protein after 48h (Figure 6C-6D). These cells were further treated with TGF–β1 (10ng/ml, 1h). In line with the MEF studies, we observed no significant effect of GSK-3α deletion on TGFβ1-induced SMAD3 phosphorylation (Figure 6E). Next, we employed a gain-of-function approach in which we used neonatal rat ventricular fibroblasts (NRVF) isolated from 1- to 3-day-old rat pups and overexpressed GSK-3α by adenoviral transduction (Ad-GSK-3α). Consistent with the loss-of-function studies, overexpression of GSK-3α had no effect on TGF-β1-induced SMAD3 activation (Figure 6F-6H). Taken together, these results suggest that CF-GSK-3α acts via eliciting SMAD3 independent pro-fibrotic signaling. We also examined the effect of GSK-3α deletion on p38α kinase, a known regulator of fibrosis that acts independently of SMAD3.[10] We found that the p38α signaling was unaffected in GSK-3α KO FBs (Figure S6).

High Throughput Profiling of GSK-3α Regulated Fibroblast Kinome Reveals downregulation of RAF kinases in KOs

To gain further clues to the fibroblast signaling pathways impacted by the knockout of GSK-3α, an unbiased kinome profiling was performed at the UAB Kinome core (https://kinomecore.com/) as described in the method section. At 4 weeks post-injury, CFs were isolated from CTL and GSK-3α^{FKO} animals and total proteins were extracted and quantified. Kinome profiling was performed on the PamStation®12 platform. Unsupervised hierarchical clustering of peptide signals was performed in BioNavigator and displayed as a heatmap demonstrating altered phosphopeptide signatures in GSK-3α^{FKO} CFs compared

to CTL (Figure 7A). Altered upstream kinases were identified within BioNavigator, highlighted by a significant reduction in phosphorylation of peptide targets of RAF family kinase, CDKs, RSKs, and AKT in GSK-3α^{FKO} CFs (Figure 7B, TableS1). These altered kinases, network-mapped against literature annotated interactions in GeneGo MetaCore led to the generation of an ERK-centric network (Figure 7C). Alterations in CDKs and AurKB kinases in kinome analysis pointed out that GSK-3α deletion might have affected the FB cell cycle. However, at 4 weeks post-TAC FB proliferation was comparable between CTL and KO groups (Figure S7). Despite no statistical significance in FB proliferation, a remarkable reduction in fibrosis was observed in KO groups at 4 weeks post-TAC. This finding further confirms that CF proliferation plays a minimal role in driving the GSK-3α mediated pro-fibrotic response.

CF-GSK-3α promotes fibrosis through the RAF-MEK-ERK signaling pathway

To validate our findings from the kinome analysis, we isolated CFs from CTL and GSK-3α^{FKO} mice post-TAC and analyzed pERK levels by western blotting and flow cytometry. As expected, we found a considerable reduction in pERK levels in GSK-3α^{FKO} mice compared to CTL at both 4 weeks and 8 weeks post-TAC (Figure 7D-7E). To examine whether GSK-3α regulates the ERK pathway under pro-fibrotic conditions, WT and GSK-3α KO fibroblasts were treated with TGF-β1 (10 ng/mL, 10min), and Western blotting was performed to determine the ERK activation. Indeed, TGF-β1-induced ERK phosphorylation was inhibited in GSK-3α KO cells (Figure 7F). We then isolated CFs from adult GSK-3α $^{fl/fl}$ mice and adenovirally transduced them with either LacZ (Ad-LacZ) as control or Cre recombinase (Ad-Cre) to delete GSK-3α, as described previously.[15] These cells were further treated with TGF–β1 (10ng/ml, 1h). In line with the MEF studies, we observed reduction in TGFβ1-induced ERK phosphorylation in GSK-3α KO CFs (Figure 7G). Next, we transfected NRVFs with adenovirus expressing a mutant form of GSK-3α (serine S21A) which cannot be phosphorylated and therefore is constitutively active. Our western blot results confirmed activation of the MEK-ERK pathway in GSK-3α overexpressing fibroblasts (Figure 8A).

A recent study has identified IL-11 as a fibroblast-specific cytokine that mediates a fibrogenic response downstream of diverse pro-fibrotic stimuli, including TGF-β1. Also, IL-11 has been demonstrated to act via an autocrine manner and is shown to cooperate with the ERK pathway to mediate fibrotic responses in FBs.[16] Since we observed that CF-GSK-3α mediates TGF-β1-induced pro-fibrotic effects independent of SMAD3, we hypothesized that GSK-3α might be interacting with the IL-11 and ERK signaling pathways to regulate fibrosis. To test this hypothesis, we first examined whether GSK-3α deletion had any effect on IL-11 levels in CFs. CFs were isolated from CTL and GSK-3α^{FKO} mice at 8 weeks post-TAC, and flow cytometry was performed to quantify the IL-11^{+ve} CFs. The flow cytometric analysis revealed a significant reduction in IL-11^{+ve} CFs in GSK-3α^{FKO} as compared to CTL mice (Figure 8B). Additionally, WT and GSK-3α KO MEFs were treated with TGF-β1 (10ng/mL, 24h) and IL-11 gene expression was determined by qPCR. GSK-3α deletion remarkably reduced basal IL-11 levels and also prevented TGF-β1-induced upregulation of IL-11 (Figure 8C). Next, we examined the effect of GSK-3α deletion on IL-11-mediated ERK activation. We treated WT and GSK-3α KO MEFs with

IL-11 (10 ng/mL, 10min) and measured pERK levels by Western blotting. Indeed, IL-11-induced ERK phosphorylation was inhibited in GSK-3α KO cells as compared to WT cells (Figure 8D).

To further examine whether GSK-3α mediates pro-fibrotic effects through the ERK pathway, we cultured control and GSK-3α overexpressing NRVFs in the presence or absence of ERK inhibitor (U0123, 10μM) for 24h. We found that GSK-3α overexpression increases the production of fibrogenic proteins (IL-11, collagen −1). Importantly this fibrotic response was blunted by ERK inhibition (Figure 8E). Taken together, these results have revealed a critical role for a GSK-3α-ERK axis in cardiac fibrosis (Figure 8F)

Discussion

In this study, we report a critical role of CF-GSK-3α in the fibrotic remodeling of failing hearts. We employed two entirely novel inducible conditional FB-specific mouse models to demonstrate that CF-specific deletion of GSK-3α prevents injury-induced myofibroblast transformation, adverse fibrotic remodeling, and deterioration of cardiac function. We found that CF-GSK-3α mediates pro-fibrotic effects independent of the canonical TGFβ1/SMAD3 pathway. Furthermore, we demonstrate a causal role of the CF GSK-3α-ERK signaling network in regulating the fibrotic response to pathological stimuli.

In cardiac fibrosis, TGFβ1/SMAD3 signaling plays a crucial role.[9, 29] Our lab has previously shown that in the ischemic heart, GSK-3β deletion aggravates fibrosis via hyperactivation of SMAD3.[15] Considering this observation, we anticipated that in the CF-GSK-3α KO heart, fibrosis might be reduced because of a direct effect of GSK-3α deletion on the TGFβ/SMAD3 pathway. To our complete surprise, GSK-3α KO CFs did not display alteration in TGFβ1-induced SMAD3 activation. This discrepancy could be explained by the well-known fact that GSK-3 isoforms play some unique biological roles despite having great sequence homology.[17] For example, global deletion of GSK-3β causes embryonic lethality while GSK-3α null animals are viable, albeit male sterile.[20, 30] Consistent with our findings, Guo et al., have demonstrated that GSK-3β, but not GSK-3α regulates the stability of non-activated SMAD3 and determines cellular sensitivity to TGFβ.[31] This evidence suggests the isoform-specific substrate preferences could be one of the reasons for the differential effect of CF-GSK-3 isoforms on the TGFβ/SMAD3 pathway.

To probe the underlying mechanisms driving the cardiac phenotype, we undertook an unbiased approach of GSK-3α regulated fibroblast kinome profiling. We found downregulation of RAF family kinases activity in GSK-3α KO CFs. The RAF-MEK-ERK pathway has been implicated in fibrotic diseases across multiple organs.[32-36] Hence, we verified whether GSK-3α interacts with ERK and whether that may have relevance in the development of cardiac fibrosis. In regard to the role of ERK in cardiac fibrosis, Thum et al. have shown that in pressure overloaded mouse heart microRNA-21 stimulates the ERK–MAP kinase signaling pathway in cardiac fibroblasts and contributes to disease pathogenesis.[37] Moreover, Schafer et al. have demonstrated that in response to a pro-fibrotic stimulus, IL-11 regulates fibrogenic protein synthesis via the ERK pathway to promote cardiac fibrosis.[16] However, there are very few reports on the interaction of GSK-3 and

ERK. An elegant study by Ding et al. group demonstrated a critical role of ERK in priming and inactivation of GSK-3β in cancer cells.[38] In the case of cardiac pathophysiology, Sadoshima's lab reported that in pressure overloaded hearts, cardiomyocyte (CM) specific GSK-3α overexpression leads to cardiac hypertrophy via inhibition of ERK, and when this inhibition is relieved by expression of constitutively active MEK1, most of the pathological features can be rescued.[39, 40] Our study suggests that CF-GSK-3α promotes fibrosis via an ERK pathway in pressure overloaded hearts and highlights a distinct fibroblast-specific response of GSK-3α under similar pathological stimuli. The precise mechanism(s) by which GSK-3α regulates ERK in fibroblasts needs further investigation. Also, studies with CF-specific ERK1/2 conditional KOs are required to precisely define the role of ERK signaling in cardiac fibroblast biology and myocardial fibrosis.

The literature available on the role of GSK-3 isoforms in cardiac diseases suggests that the consequences of cardiac-specific GSK-3β manipulation are complex and context-dependent.[15, 18-21] However, GSK-3α deletion has consistently shown cardioprotection irrespective of pathological stimuli.[41] Our lab has reported that the CM-specific deletion of GSK-3α limits adverse remodeling and improves cardiac function post-MI.[25] Furthermore, our lab has demonstrated that the CM-specific deletion of GSK-3α protects from pressure overload-induced LV remodeling and cardiac dysfunction.[24] Additionally, the critical contribution of GSK-3α to pathological cardiac hypertrophy is recapitulated in the gain of function studies by employing transgenic and KI mouse models.[19, 40] Consistent with all of these studies, here we report the beneficial effects of fibroblast-specific GSK-3α deletion against pressure overload-induced cardiac damages. Taken together, these pre-clinical data provide of proof-of-concept that selective therapeutic inhibition of GSK-3α could be a viable target for heart failure management.

In summary, we report that CF-specific deletion of GSK-3α prevents adverse fibrotic remodeling and improves the function of the diseased heart. Mechanistically, we have demonstrated for the first time that in response to pro-fibrotic stimuli, GSK-3α cooperates with the ERK pathway to mediate the fibrogenic response. Clinically, given the findings of the present study and the literature discussed above, selectively targeting GSK-3α could be a novel and safe strategy to limit cardiac fibrosis and heart failure.

Supplementary Material

Refer to Web version on PubMed Central for supplementary material.

Sources of funding

This work was supported by research grants from the NHLBI (R01HL133290) to HL, PU was supported by American Heart Association (19POST34460025).

NON-STANDARD ABBREVIATIONS AND ACRONYMS:

CF	Cardiac Fibroblast
FB	Fibroblast

NRVF	Neonatal Rat Ventricular Fibroblast
CSA	Cross-Sectional Area
HW	Heart weight
LV	Left Ventricle
LW	Lung weight
MCM	Mer-Cre-Mer
TAM	Tamoxifen
TL	Tibia length

References

1. Zannad F, Rossignol P and Iraqi W. Extracellular matrix fibrotic markers in heart failure. Heart Fail Rev. 2010;15:319–29. [PubMed: 19404737]
2. Radauceanu A, Ducki C, Virion JM, Rossignol P, Mallat Z, McMurray J, Van Veldhuisen DJ, Tavazzi L, Mann DL, Capiaumont-Vin J, Li M, Hanriot D and Zannad F. Extracellular matrix turnover and inflammatory markers independently predict functional status and outcome in chronic heart failure. J Card Fail. 2008;14:467–74. [PubMed: 18672194]
3. Zannad F, Alla F, Dousset B, Perez A and Pitt B. Limitation of excessive extracellular matrix turnover may contribute to survival benefit of spironolactone therapy in patients with congestive heart failure: insights from the randomized aldactone evaluation study (RALES). Rales Investigators. Circulation. 2000;102:2700–6. [PubMed: 11094035]
4. Pinto AR, Ilinykh A, Ivey MJ, Kuwabara JT, D'Antoni ML, Debuque R, Chandran A, Wang L, Arora K, Rosenthal NA and Tallquist MD. Revisiting Cardiac Cellular Composition. Circ Res. 2016;118:400–9. [PubMed: 26635390]
5. Weber KT, Sun Y, Bhattacharya SK, Ahokas RA and Gerling IC. Myofibroblast-mediated mechanisms of pathological remodelling of the heart. Nat Rev Cardiol. 2013;10:15–26. [PubMed: 23207731]
6. Guo Y, Gupte M, Umbarkar P, Singh AP, Sui JY, Force T and Lal H. Entanglement of GSK-3beta, beta-catenin and TGF-beta1 signaling network to regulate myocardial fibrosis. J Mol Cell Cardiol. 2017;110:109–120. [PubMed: 28756206]
7. Fu X, Khalil H, Kanisicak O, Boyer JG, Vagnozzi RJ, Maliken BD, Sargent MA, Prasad V, Valiente-Alandi I, Blaxall BC and Molkentin JD. Specialized fibroblast differentiated states underlie scar formation in the infarcted mouse heart. J Clin Invest. 2018;128:2127–2143. [PubMed: 29664017]
8. Xiang FL, Fang M and Yutzey KE. Loss of beta-catenin in resident cardiac fibroblasts attenuates fibrosis induced by pressure overload in mice. Nat Commun. 2017;8:712. [PubMed: 28959037]
9. Khalil H, Kanisicak O, Prasad V, Correll RN, Fu X, Schips T, Vagnozzi RJ, Liu R, Huynh T, Lee SJ, Karch J and Molkentin JD. Fibroblast-specific TGF-beta-Smad2/3 signaling underlies cardiac fibrosis. J Clin Invest. 2017;127:3770–3783. [PubMed: 28891814]
10. Molkentin JD, Bugg D, Ghearing N, Dorn LE, Kim P, Sargent MA, Gunaje J, Otsu K and Davis J. Fibroblast-Specific Genetic Manipulation of p38 Mitogen-Activated Protein Kinase In Vivo Reveals Its Central Regulatory Role in Fibrosis. Circulation. 2017;136:549–561. [PubMed: 28356446]
11. Kanisicak O, Khalil H, Ivey MJ, Karch J, Maliken BD, Correll RN, Brody MJ, SC JL, Aronow BJ, Tallquist MD and Molkentin JD. Genetic lineage tracing defines myofibroblast origin and function in the injured heart. Nat Commun. 2016;7:12260. [PubMed: 27447449]
12. Acharya A, Baek ST, Banfi S, Eskiocak B and Tallquist MD. Efficient inducible Cre-mediated recombination in Tcf21 cell lineages in the heart and kidney. Genesis. 2011;49:870–7. [PubMed: 21432986]

13. Snider JC, Riley LA, Mallory NT, Bersi MR, Umbarkar P, Gautam R, Zhang Q, Mahadevan-Jansen A, Hatzopoulos AK, Maroteaux L, Lal H and Merryman WD. Targeting 5-HT2B Receptor Signaling Prevents Border Zone Expansion and Improves Microstructural Remodeling after Myocardial Infarction. Circulation. 2021.
14. Derynck R and Zhang YE. Smad-dependent and Smad-independent pathways in TGF-beta family signalling. Nature. 2003;425:577–84. [PubMed: 14534577]
15. Lal H, Ahmad F, Zhou J, Yu JE, Vagnozzi RJ, Guo Y, Yu D, Tsai EJ, Woodgett J, Gao E and Force T. Cardiac fibroblast glycogen synthase kinase-3beta regulates ventricular remodeling and dysfunction in ischemic heart. Circulation. 2014;130:419–30. [PubMed: 24899689]
16. Schafer S, Viswanathan S, Widjaja AA, Lim WW, Moreno-Moral A, DeLaughter DM, Ng B, Patone G, Chow K, Khin E, Tan J, Chothani SP, Ye L, Rackham OJL, Ko NSJ, Sahib NE, Pua CJ, Zhen NTG, Xie C, Wang M, Maatz H, Lim S, Saar K, Blachut S, Petretto E, Schmidt S, Putoczki T, Guimaraes-Camboa N, Wakimoto H, van Heesch S, Sigmundsson K, Lim SL, Soon JL, Chao VTT, Chua YL, Tan TE, Evans SM, Loh YJ, Jamal MH, Ong KK, Chua KC, Ong BH, Chakaramakkil MJ, Seidman JG, Seidman CE, Hubner N, Sin KYK and Cook SA. IL-11 is a crucial determinant of cardiovascular fibrosis. Nature. 2017;552:110–115. [PubMed: 29160304]
17. Lal H, Ahmad F, Woodgett J and Force T. The GSK-3 family as therapeutic target for myocardial diseases. Circ Res. 2015;116:138–49. [PubMed: 25552693]
18. Woulfe KC, Gao E, Lal H, Harris D, Fan Q, Vagnozzi R, DeCaul M, Shang X, Patel S, Woodgett JR, Force T and Zhou J. Glycogen synthase kinase-3beta regulates post-myocardial infarction remodeling and stress-induced cardiomyocyte proliferation in vivo. Circ Res. 2010;106:1635–45. [PubMed: 20360256]
19. Matsuda T, Zhai P, Maejima Y, Hong C, Gao S, Tian B, Goto K, Takagi H, Tamamori-Adachi M, Kitajima S and Sadoshima J. Distinct roles of GSK-3alpha and GSK-3beta phosphorylation in the heart under pressure overload. Proc Natl Acad Sci U S A. 2008;105:20900–5. [PubMed: 19106302]
20. Kerkela R, Kockeritz L, Macaulay K, Zhou J, Doble BW, Beahm C, Greytak S, Woulfe K, Trivedi CM, Woodgett JR, Epstein JA, Force T and Huggins GS. Deletion of GSK-3beta in mice leads to hypertrophic cardiomyopathy secondary to cardiomyoblast hyperproliferation. J Clin Invest. 2008;118:3609–18. [PubMed: 18830417]
21. Haq S, Choukroun G, Kang ZB, Ranu H, Matsui T, Rosenzweig A, Molkentin JD, Alessandrini A, Woodgett J, Hajjar R, Michael A and Force T. Glycogen synthase kinase-3beta is a negative regulator of cardiomyocyte hypertrophy. J Cell Biol. 2000;151:117–30. [PubMed: 11018058]
22. Nakamura M, Liu T, Husain S, Zhai P, Warren JS, Hsu CP, Matsuda T, Phiel CJ, Cox JE, Tian B, Li H and Sadoshima J. Glycogen Synthase Kinase-3alpha Promotes Fatty Acid Uptake and Lipotoxic Cardiomyopathy. Cell Metab. 2019;29:1119–1134 e12. [PubMed: 30745182]
23. Cho J, Rameshwar P and Sadoshima J. Distinct roles of glycogen synthase kinase (GSK)-3alpha and GSK-3beta in mediating cardiomyocyte differentiation in murine bone marrow-derived mesenchymal stem cells. J Biol Chem. 2009;284:36647–36658. [PubMed: 19858210]
24. Ahmad F, Singh AP, Tomar D, Rahmani M, Zhang Q, Woodgett JR, Tilley DG, Lal H and Force T. Cardiomyocyte-GSK-3alpha promotes mPTP opening and heart failure in mice with chronic pressure overload. J Mol Cell Cardiol. 2019;130:65–75. [PubMed: 30928428]
25. Ahmad F, Lal H, Zhou J, Vagnozzi RJ, Yu JE, Shang X, Woodgett JR, Gao E and Force T. Cardiomyocyte-specific deletion of Gsk3alpha mitigates post-myocardial infarction remodeling, contractile dysfunction, and heart failure. J Am Coll Cardiol. 2014;64:696–706. [PubMed: 25125302]
26. Acharya A, Baek ST, Huang G, Eskiocak B, Goetsch S, Sung CY, Banfi S, Sauer MF, Olsen GS, Duffield JS, Olson EN and Tallquist MD. The bHLH transcription factor Tcf21 is required for lineage-specific EMT of cardiac fibroblast progenitors. Development. 2012;139:2139–49. [PubMed: 22573622]
27. Zhou J, Freeman TA, Ahmad F, Shang X, Mangano E, Gao E, Farber J, Wang Y, Ma XL, Woodgett J, Vagnozzi RJ, Lal H and Force T. GSK-3alpha is a central regulator of age-related pathologies in mice. J Clin Invest. 2013;123:1821–32. [PubMed: 23549082]
28. Zhai P, Sciarretta S, Galeotti J, Volpe M and Sadoshima J. Differential roles of GSK-3beta during myocardial ischemia and ischemia/reperfusion. Circ Res. 2011;109:502–11. [PubMed: 21737790]

29. Dobaczewski M, Bujak M, Li N, Gonzalez-Quesada C, Mendoza LH, Wang XF and Frangogiannis NG. Smad3 signaling critically regulates fibroblast phenotype and function in healing myocardial infarction. Circ Res. 2010;107:418–28. [PubMed: 20522804]
30. Lal H, Zhou J, Ahmad F, Zaka R, Vagnozzi RJ, Decaul M, Woodgett J, Gao E and Force T. Glycogen synthase kinase-3alpha limits ischemic injury, cardiac rupture, post-myocardial infarction remodeling and death. Circulation. 2012;125:65–75. [PubMed: 22086876]
31. Guo X, Ramirez A, Waddell DS, Li Z, Liu X and Wang XF. Axin and GSK3-control Smad3 protein stability and modulate TGF- signaling. Genes & development. 2008;22:106–20. [PubMed: 18172167]
32. Weng CH, Li YJ, Wu HH, Liu SH, Hsu HH, Chen YC, Yang CW, Chu PH and Tian YC. Interleukin-17A induces renal fibrosis through the ERK and Smad signaling pathways. Biomed Pharmacother. 2020;123:109741. [PubMed: 31901549]
33. Hu Y, Fu J and Xue X. Association of the proliferation of lung fibroblasts with the ERK1/2 signaling pathway in neonatal rats with hyperoxia-induced lung fibrosis. Exp Ther Med. 2019;17:701–708. [PubMed: 30651853]
34. Chen HY, Lin CH and Chen BC. ADAM17/EGFR-dependent ERK activation mediates thrombin-induced CTGF expression in human lung fibroblasts. Exp Cell Res. 2018;370:39–45. [PubMed: 29902535]
35. Ghatak S, Markwald RR, Hascall VC, Dowling W, Lottes RG, Baatz JE, Beeson G, Beeson CC, Perrella MA, Thannickal VJ and Misra S. Transforming growth factor beta1 (TGFbeta1) regulates CD44V6 expression and activity through extracellular signal-regulated kinase (ERK)-induced EGR1 in pulmonary fibrogenic fibroblasts. J Biol Chem. 2017;292:10465–10489. [PubMed: 28389562]
36. Wong VW, Rustad KC, Akaishi S, Sorkin M, Glotzbach JP, Januszyk M, Nelson ER, Levi K, Paterno J, Vial IN, Kuang AA, Longaker MT and Gurtner GC. Focal adhesion kinase links mechanical force to skin fibrosis via inflammatory signaling. Nat Med. 2011;18:148–52. [PubMed: 22157678]
37. Thum T, Gross C, Fiedler J, Fischer T, Kissler S, Bussen M, Galuppo P, Just S, Rottbauer W, Frantz S, Castoldi M, Soutschek J, Koteliansky V, Rosenwald A, Basson MA, Licht JD, Pena JT, Rouhanifard SH, Muckenthaler MU, Tuschl T, Martin GR, Bauersachs J and Engelhardt S. MicroRNA-21 contributes to myocardial disease by stimulating MAP kinase signalling in fibroblasts. Nature. 2008;456:980–4. [PubMed: 19043405]
38. Ding Q, Xia W, Liu JC, Yang JY, Lee DF, Xia J, Bartholomeusz G, Li Y, Pan Y, Li Z, Bargou RC, Qin J, Lai CC, Tsai FJ, Tsai CH and Hung MC. Erk associates with and primes GSK-3beta for its inactivation resulting in upregulation of beta-catenin. Mol Cell. 2005;19:159–70. [PubMed: 16039586]
39. Maejima Y, Galeotti J, Molkentin JD, Sadoshima J and Zhai P. Constitutively active MEK1 rescues cardiac dysfunction caused by overexpressed GSK-3alpha during aging and hemodynamic pressure overload. American journal of physiology Heart and circulatory physiology. 2012;303:H979–88. [PubMed: 22904158]
40. Zhai P, Gao S, Holle E, Yu X, Yatani A, Wagner T and Sadoshima J. Glycogen synthase kinase-3alpha reduces cardiac growth and pressure overload-induced cardiac hypertrophy by inhibition of extracellular signal-regulated kinases. J Biol Chem. 2007;282:33181–91. [PubMed: 17855351]
41. Ahmad F and Woodgett JR. Emerging roles of GSK-3alpha in pathophysiology: Emphasis on cardio-metabolic disorders. Biochim Biophys Acta Mol Cell Res. 2020;1867:118616. [PubMed: 31785335]

Novelty and Significance

What Is Known?

- Irrespective of the underlying cause, heart disease is often associated with fibroblast (FB) activation and myocardial fibrosis, which stiffens the heart and leads to adverse cardiac remodeling.
- GSK-3 isoforms have been implicated as potential therapeutic targets for cardiovascular diseases.
- Among the two GSK-3 isoforms, GSK-3β acts as a negative regulator of myocardial fibrosis in the diseased heart. However, the role of GSK-3α in fibroblast biology and myocardial fibrosis is unknown.

What New Information Does This Article Contribute?

- We discovered significant activation of GSK-3α in cardiac FBs in stressed hearts.
- FB-specific deletion of GSK-3α attenuated fibroblast activation and myocardial fibrosis and preserved the cardiac structural integrity and function.
- We identified a novel GSK-3α-MEK-ERK-IL-11 signaling circuit as a potent profibrotic pathway operational in stressed hearts.

Fibroblast activation and excessive fibrosis are integral to many forms of heart disease. Activated fibroblasts are the critical driver of adverse fibrotic remodeling by depositing extracellular matrix (ECM), the main component of excessive fibrosis. Since the molecular mechanisms of cardiac fibrosis are largely unknown, there is no specific therapeutic strategy to combat adverse myocardial fibrotic remodeling. This study establishes the GSK-3α as a potential target for limiting fibroblast activation and adverse fibrotic remodeling of a diseased heart. Based on multiple conditional FB-specific loss of function models, we demonstrate that GSK-3α promotes fibroblast activation and excessive fibrosis culminating in cardiac dysfunction and heart failure. Mechanistically, we discovered the GSK-3α-MEK-ERK-IL-11 signaling circuit as a novel profibrotic pathway in stressed hearts suggesting thatits inhibition may be a potential therapeutic strategy to combat myocardial fibrosis.

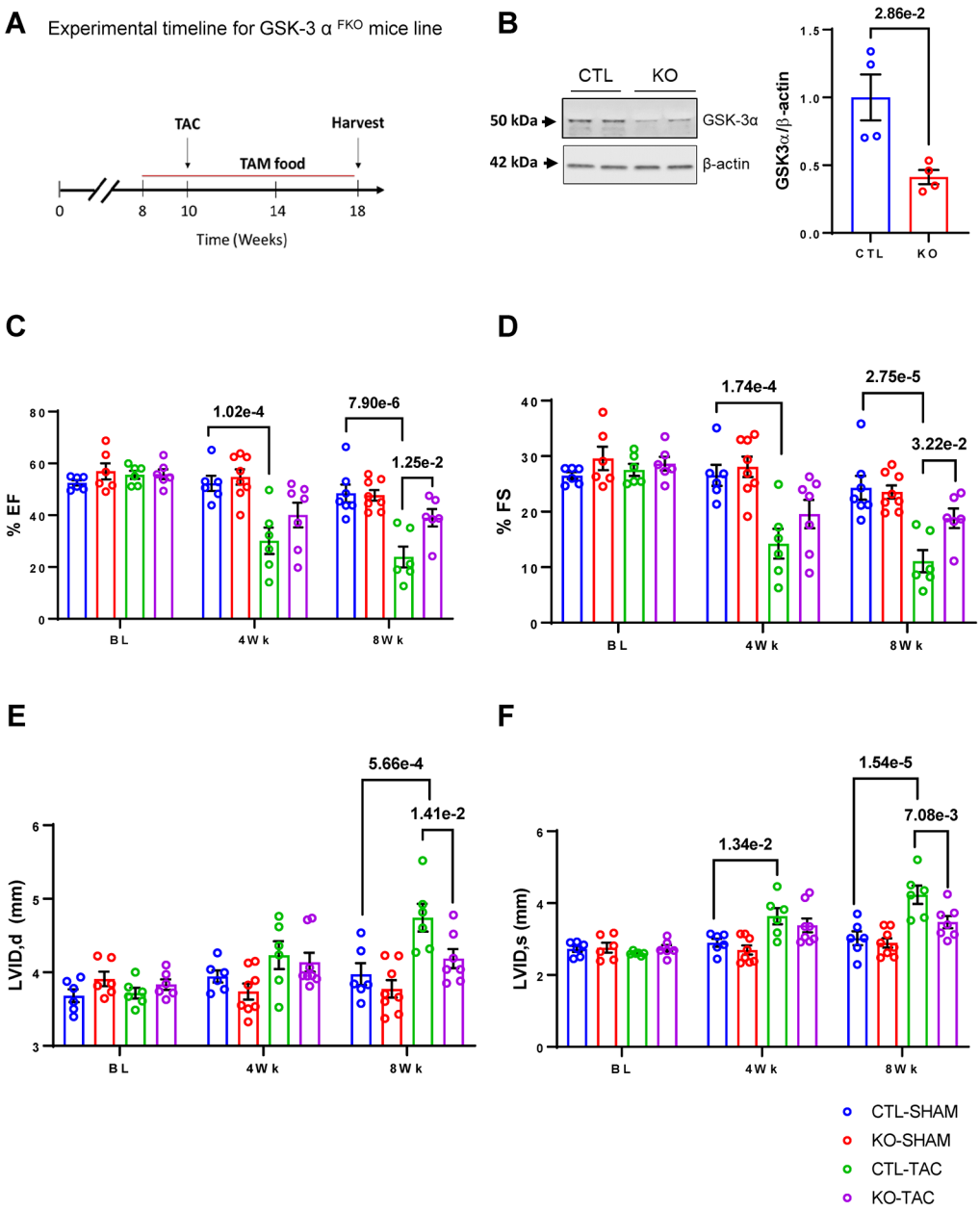

Figure 1: Deletion of CF-GSK-3α from resident cardiac fibroblasts prevents pressure overload-induced cardiac dysfunction

(A) Experimental design. Two-month-old mice were fed tamoxifen (TAM) chow diet. After 2 weeks of TAM treatment, mice were subjected to TAC surgery and are maintained on the TAM diet till the end of the study. **(B)** Western blot analysis of GSK-3α protein levels in cardiac fibroblasts after TAM treatment. N=4 per group. Data were analyzed using the Mann-Whitney test and represented as mean ± SEM. Evaluation of cardiac function by m-mode echocardiography; **(C)** Ejection fraction (EF), **(D)** Fractional shortening (FS), For C and D – At BL, (N=6) per group. At 4 weeks, CTL-SHAM & CTL-TAC (N=6), KO-SHAM (N=8), and KO-TAC (N=7). At 8 weeks, CTL-SHAM (N=7), KO-SHAM (N=8), CTL-TAC & KO-TAC (N=6). **(E)** LV end-diastolic interior dimension (LVID;d) and **(F)**

LV end-systolic interior dimension (LVID;s). For E and F – At BL, (N=6) per group. At 4 weeks, CTL-SHAM & CTL-TAC (N=6), KO-SHAM & KO-TAC (N=8). At 8 weeks, CTL-SHAM & CTL-TAC (N=6), KO-SHAM (N=8), and KO-TAC (N=7). Data **(1C-1F)** were analyzed using Two-way ANOVA followed by Tukey's *post hoc* analysis and represented as mean ± SEM. BL: Baseline

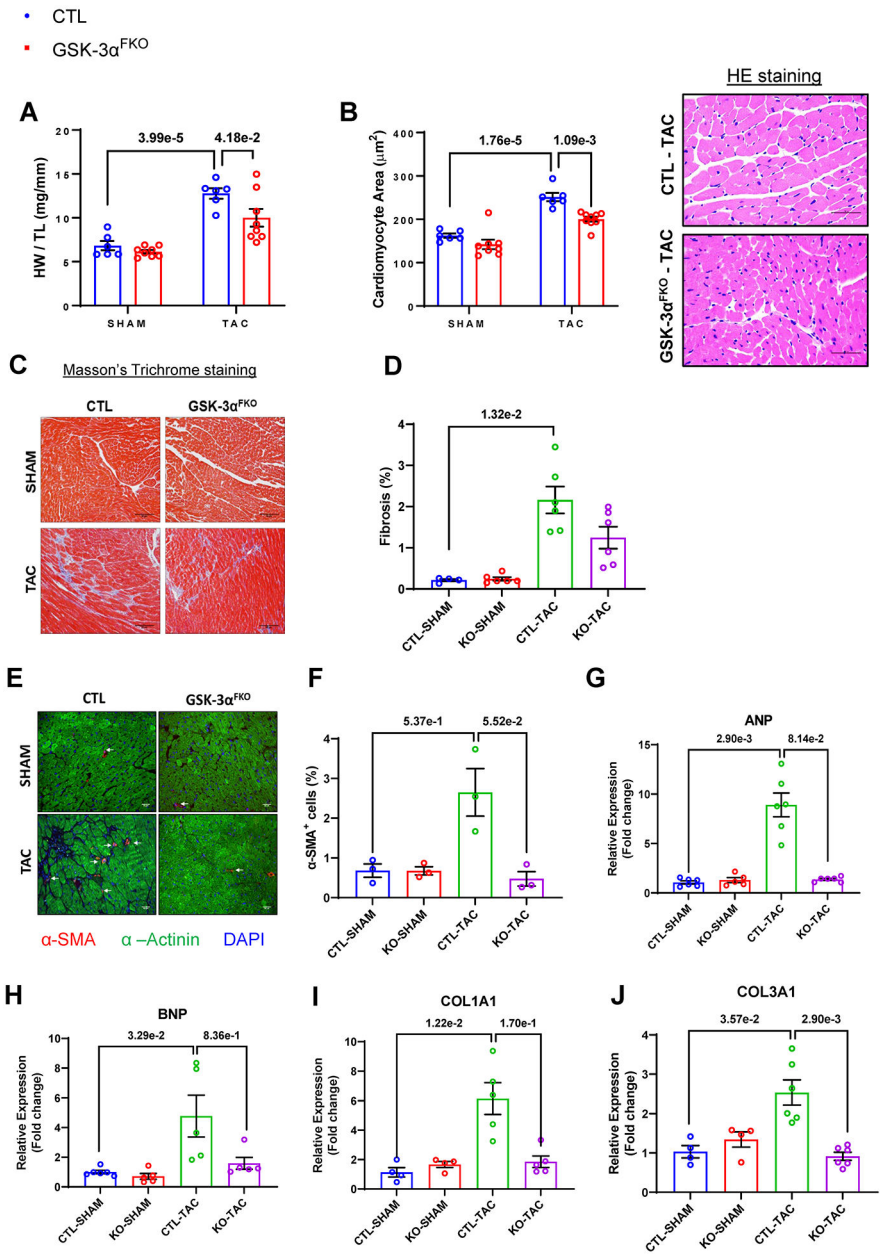

Figure 2: Deletion of CF-GSK-3α from resident cardiac fibroblasts prevents pressure overload-induced adverse cardiac remodeling

Morphometric studies were performed 8 weeks after TAC surgery. Assessment of cardiac hypertrophy; **(A)** Heart weight (HW) to tibia length (TL) ratio, CTL-SHAM & CTL-TAC (N=6), KO-SHAM & KO-TAC (N=8), and **(B)** Quantification of cardiomyocyte cross-sectional area (CSA) CTL-SHAM & CTL-TAC (N=6), KO-SHAM (N=8), KO-TAC (N=9) and Representative images of HE staining. Data **(2A-2B)** were analyzed using Two-way ANOVA followed by Tukey's *post hoc* analysis and represented as mean ± SEM. Assessment of cardiac fibrosis by Masson's Trichrome staining; **(C)** Representative Trichrome-stained LV regions and **(D)** Quantification of LV fibrosis. CTL-SHAM (N=4), KO-SHAM, CTL-TAC & KO-TAC (N=6) **(E)** Representative images of α-SMA staining,

white arrows indicate α-SMA^{+ve} non-vascular cells, and, **(F)** Quantification of α-SMA^{+ve} non-vascular cells. Scale bar = 30 μm. N=3 per group. RNA was extracted from the left ventricle of experimental animals, and gene expression analysis was carried out by qPCR; The gene expression from each group was normalized to the CTL-SHAM group; **(G)** ANP, CTL-SHAM, CTL-TAC, & KO-TAC (N=6), KO-SHAM (N=5), **(H)** BNP, CTL-SHAM (N=6), KO-SHAM, CTL-TAC & KO-TAC (N=5) **(I)** COL1A1, CTL-SHAM & KO-SHAM (N=4), CTL-TAC & KO-TAC (N=5) and **(J)** COL3A1, CTL-SHAM & KO-SHAM (N=4), CTL-TAC & KO-TAC (N=6). Data **(2D, 2F-2J)** were analyzed using Kruskal-Wallis followed by Dunn test and represented as mean ± SEM.

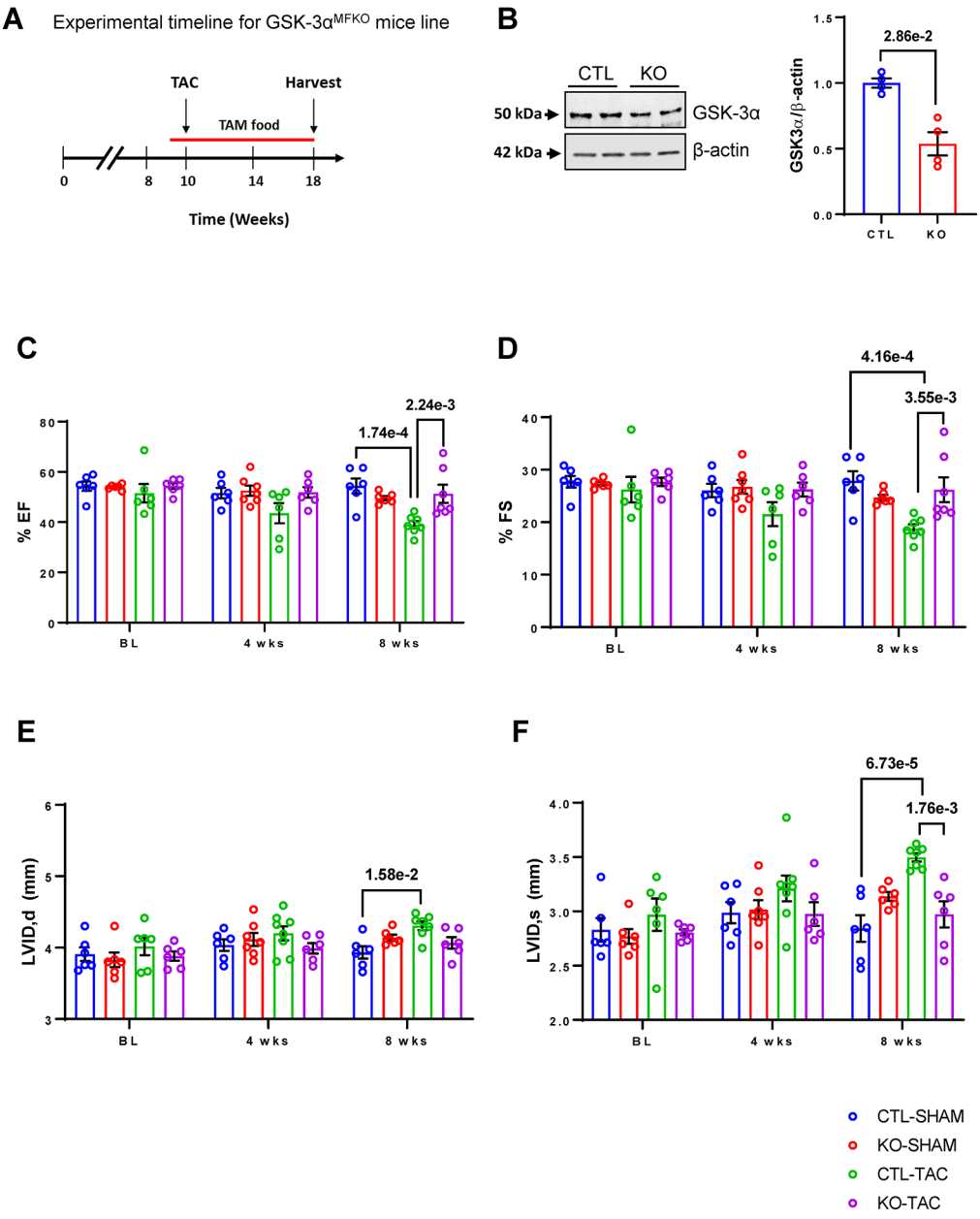

Figure 3: Deletion of CF-GSK-3α from myofibroblasts prevents pressure overload-induced cardiac dysfunction

(A) Experimental design. Two-month-old mice were fed tamoxifen (TAM) chow diet. After 1 week of TAM treatment, mice were subjected to TAC surgery and are maintained on the TAM diet till the end of the study. **(B)** Western blot analysis of GSK-3α protein levels in cardiac fibroblasts after TAM treatment. N=4 per group. Data were analyzed using the Mann-Whitney test and represented as mean ± SEM. Evaluation of cardiac function by m-mode echocardiography; **(C)** Ejection fraction (EF), **(D)** Fractional shortening (FS), For C and D – At BL, N=6 per group. At 4 weeks, CTL-SHAM, CTL-TAC & KO-TAC (N=6), KO-SHAM (N=7). At 8 weeks, CTL-SHAM & KO-SHAM (N=6), CTL-TAC & KO-TAC (N=7). **(E)** LV end-diastolic interior dimension (LVID;d) and **(F)** LV end-systolic interior

dimension (LVID;s). For E and F – At BL, N=6 per group. At 4 weeks, CTL-SHAM & KO-TAC (N=6), KO-SHAM (N=7), and CTL-TAC (N=8). At 8 weeks, CTL-SHAM, KO-SHAM & KO-TAC (N=6), CTL-TAC (N=7). Data **(3C-3F)** were analyzed using Two-way ANOVA followed by Tukey's *post hoc* analysis and represented as mean ± SEM. BL: Baseline

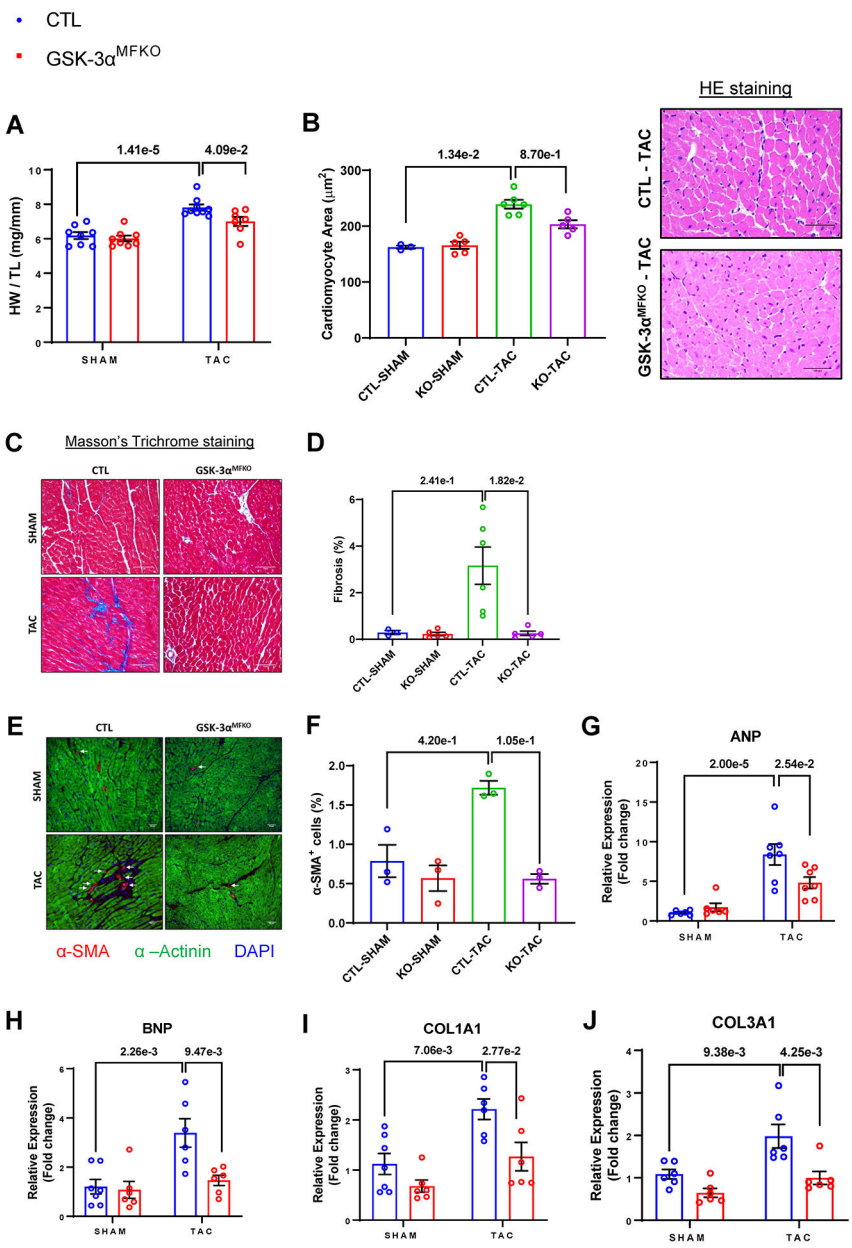

Figure 4: Deletion of CF-GSK-3α from myofibroblasts prevents pressure overload-induced adverse cardiac remodeling

Morphometric studies were performed 8 weeks after TAC surgery. Assessment of cardiac hypertrophy; **(A)** Heart weight (HW) to tibia length (TL) ratio, CTL-SHAM & KO-SHAM (N=8), CTL-TAC (N=9), KO-TAC (N=7). **(B)** Quantification of cardiomyocyte cross-sectional area (CSA) and Representative images of HE staining. Assessment of cardiac fibrosis by Masson's Trichrome staining; **(C)** Representative Trichrome-stained LV regions and **(D)** Quantification of LV fibrosis. CTL-SHAM (N=3), KO-SHAM & KO-TAC (N=5), CTL-TAC (N=6) **(E)** Representative images of α-SMA staining, white arrows indicate α-SMA^{+ve} non-vascular cells and, **(F)** Quantification of α-SMA^{+ve} non-vascular cells. Scale bar = 30 μm. N=3 per group. RNA was extracted from the left ventricle of experimental

animals, and gene expression analysis was carried out by qPCR; The gene expression from each group was normalized to the CTL-SHAM group; **(G)** ANP, CTL-SHAM & KO-SHAM (N=6), CTL-TAC & KO-TAC (N=7) **(H)** BNP, CTL-SHAM (N=7), KO-SHAM, CTL-TAC & KO-TAC (N=6) **(I)** COL1A1, CTL-SHAM (N=6), KO-SHAM, CTL-TAC & KO-TAC (N=6) and **(J)** COL3A1, N=6 per group. Data **(4B, 4D, 4F)** were analyzed using Kruskal-Wallis followed by Dunn test and represented as mean ± SEM. Data **(4A, 4G-4J)** were analyzed using Two-way ANOVA followed by Tukey's *post hoc* analysis and represented as mean ± SEM.

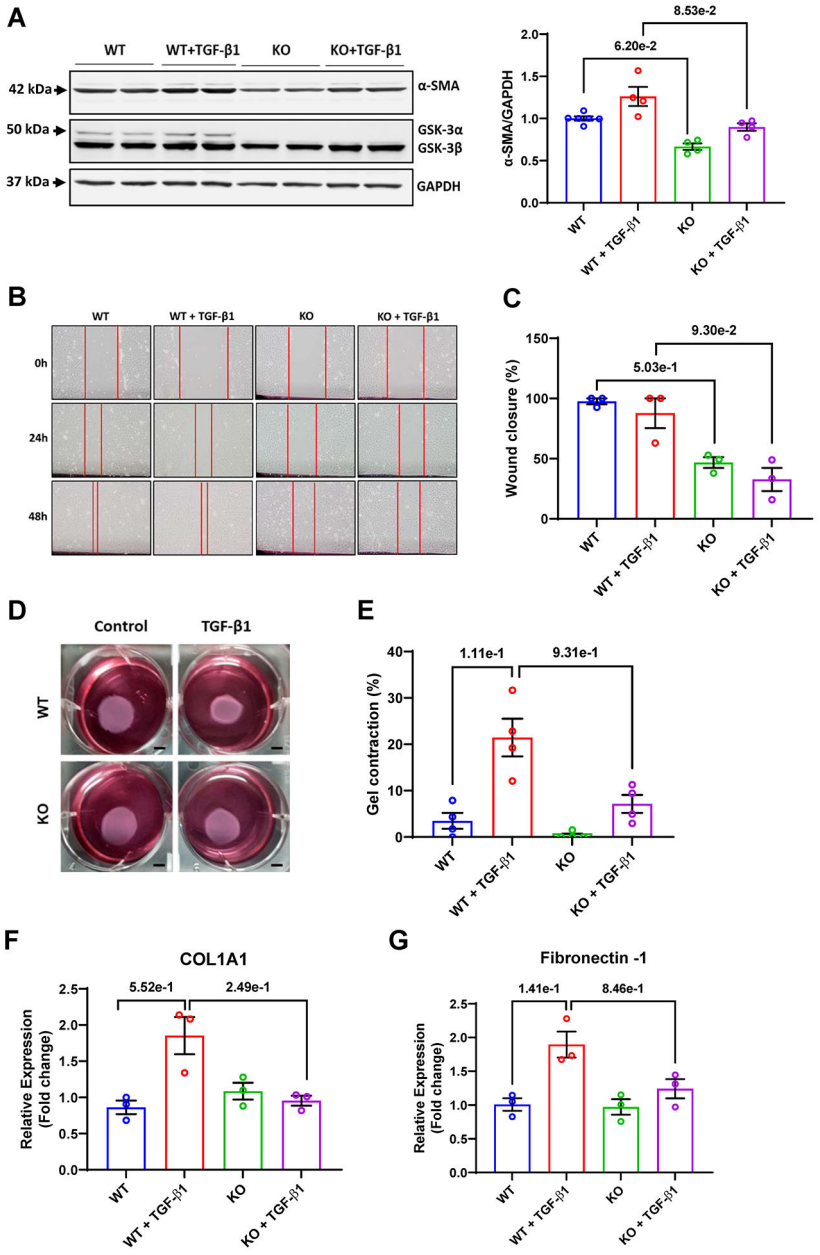

Figure 5: CF-GSK-3α regulates TGF-β1-induced myofibroblast transformation

WT and GSK-3α KO mouse embryonic fibroblasts (MEFs) were treated with TGF-β1 (10 ng/mL). **(A)** Western blot analysis of α-SMA protein levels after 48h of TGFβ1 treatment; Representative blot and quantification WT(N=6), WT + TGFβ1, KO & KO + TGFβ1 (N=4). For wound closure assay, WT and GSK-3α KO MEFs were seeded and grown till confluency. A scratch was made followed by TGF-β1 (10 ng/mL) treatment, and wound closure was monitored; **(B)** Representative images and **(C)** Quantification of wound closure at 48h, N=3 per group. For gel contraction assay, collagen gels were populated with WT and GSK-3α KO MEFs followed by TGF-β1 (10 ng/mL) treatment. % Gel contraction was calculated after 48h of TGFβ1 treatment; **(D)** Representative image and **(E)** Quantification of gel contraction, N = 4 per group. RNA was extracted from cells after 24h of TGFβ1

treatment, and gene expression analysis was carried out by the qPCR method; the gene expression from each group was normalized to the WT group. For F and G, N=3 per group, **(F)** COL1A1, **(G)** Fibronectin −1. Data **(5A, 5C, 5E-5G)** were analyzed using Kruskal-Wallis followed by Dunn test and represented as mean ± SEM.

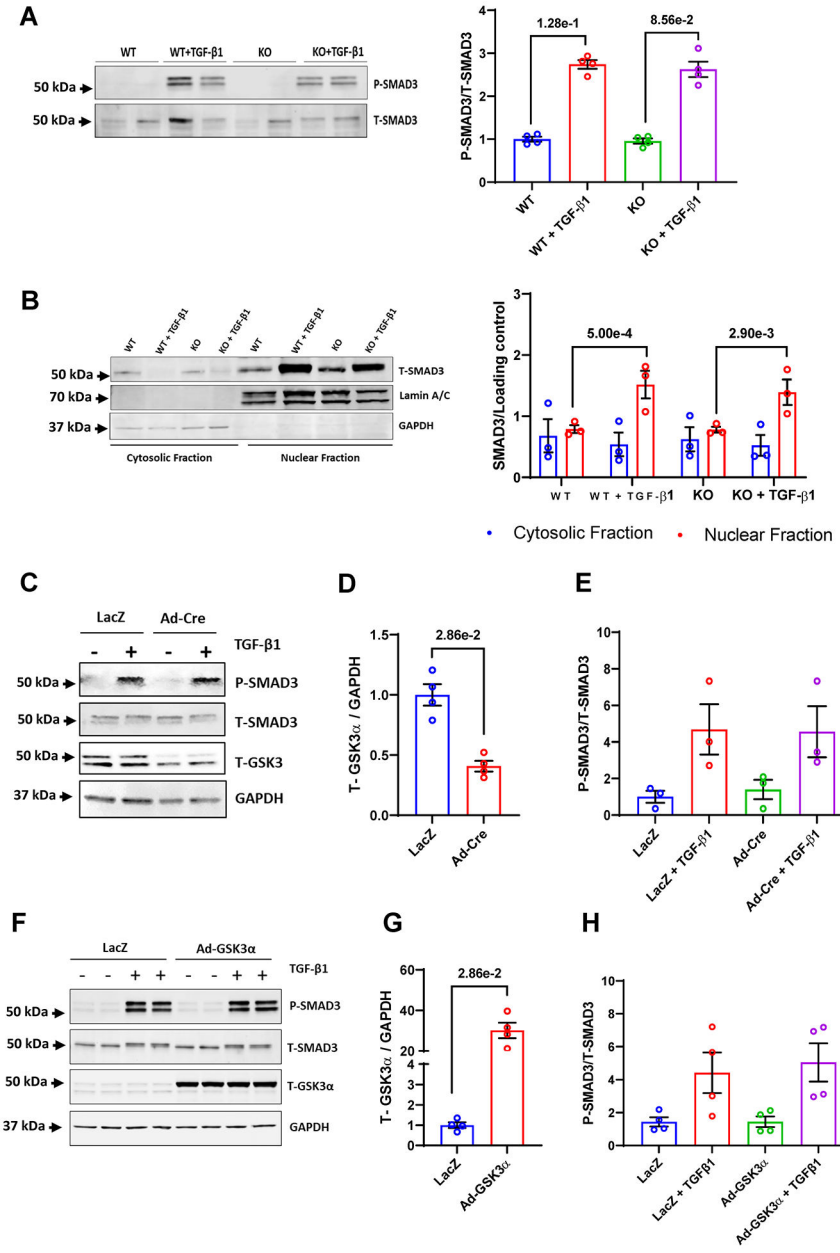

Figure 6: CF-GSK-3α mediates pro-fibrotic effects independent of SMAD3

WT and GSK-3α KO MEFs were treated with TGF-β1 (10 ng/mL) for 1h. Western blot analysis of SMAD3 phosphorylation; **(A)** Representative blot and quantification. Additionally, nuclear-cytoplasmic extraction was carried out and SMAD3 protein levels were analyzed by Western blotting; **(B)** Representative blot, and quantification. For loss of function studies, CFs were isolated from adult GSK-3α$^{fl/fl}$ mice and GSK-3α was deleted by adenoviral expression of Cre. After transduction, CFs were treated with TGF-β1 (10 ng/mL) for 1h. Western blotting was carried out; **(C)** Representative Western blot, and quantification of **(D)** GSK-3α and **(E)** SMAD3. For gain-of-function studies, GSK-3α was overexpressed in neonatal rat ventricular fibroblasts (NRVFs), and cells were treated with TGF-β1 (10 ng/mL, 1h). Western blotting was carried out; **(F)** Representative Western blot,

and quantification of **(G)** GSK-3α and **(H)** SMAD3. N=3 per group for B & E; N=4 per group for A, D, G & H. Data **(6A, 6B, 6E, 6H)** were analyzed by Kruskal-Wallis followed by Dunn test and represented as mean ± SEM. Data **(6D & 6G)** were analyzed using the Mann-Whitney test and represented as mean ± SEM.

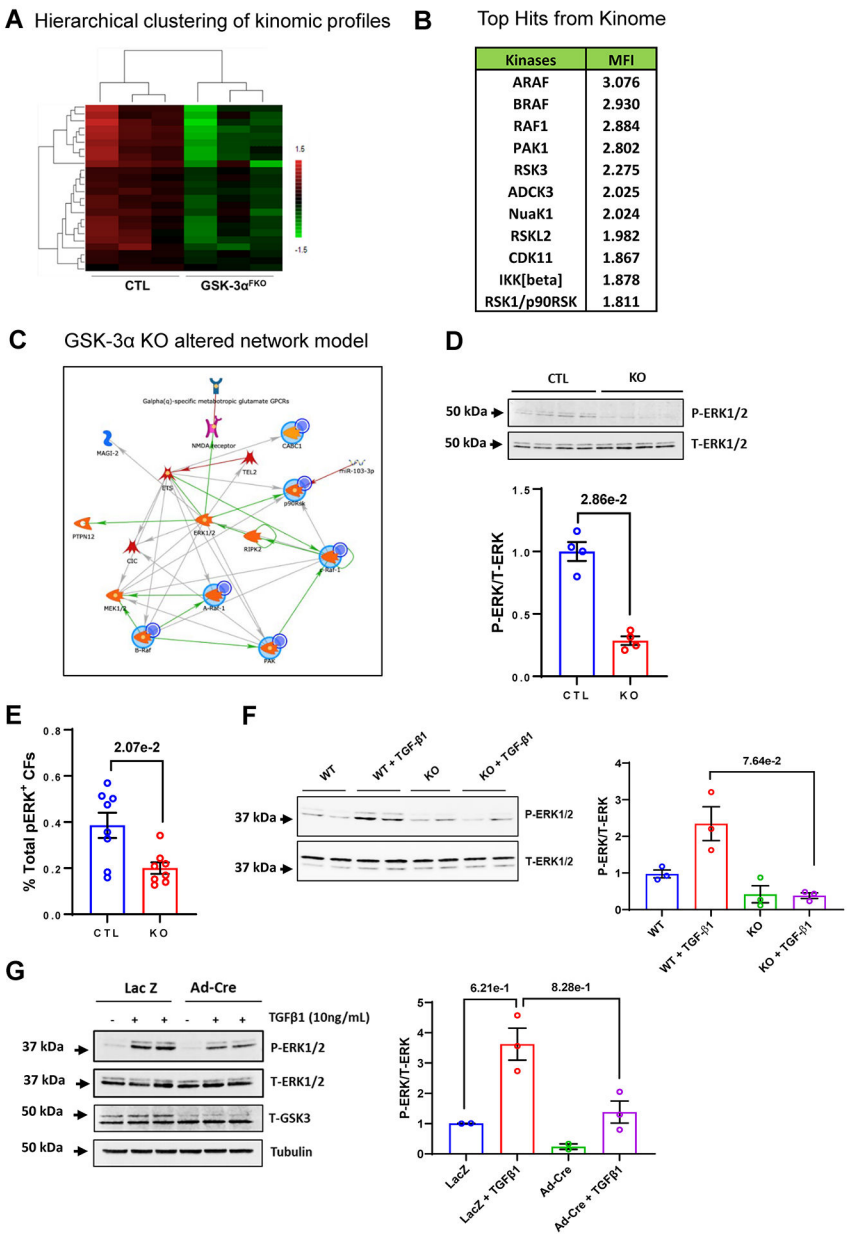

Figure 7: CF-GSK-3α promotes fibrosis through the RAF-MEK-ERK signaling network

At 4 weeks post-TAC, proteins were extracted from CFs of CTL and GSK-3α^{FKO} mice, and comparative kinome profiling was carried out; **(A)** A hierarchically-clustered heatmap of kinomic peptide phosphorylation signal intensity (change from mean) demonstrates CTL and GSK-3α KO signatures **(B)** Table displays the BioNavigator generated Mean Final Score of GSK-3α KO altered kinases **(C)** that are mapped to the literature annotated ERK centric network model. N=3 per group. Input nodes (kinases) have large blue circles around them, with smaller circles in the top right. Arrowheads denote the direction of interaction, and the color of the lines indicates the type of interaction (green: positive, red: inhibitory, grey: complex). **(D)** At 4 weeks post-TAC, CFs were isolated from CTL and GSK-3α^{FKO} mice. ERK levels were analyzed by western blotting. Representative western

blot and quantification. N=4 per group. **(E)** At 8 weeks post-TAC, CFs were isolated from CTL and GSK-3α^{FKO} mice. Flow cytometric analysis of pERK^{+ve} CFs (% total). N=8 per group. **(F)** WT and GSK-3α KO MEFs were treated with TGF-β1 (10 ng/mL) for 10 min and ERK levels were assessed by Western blotting. Representative blot and quantification, N=3 per group. The original order of lanes was rearranged to make the final representative image. **(G)** For loss of function studies, CFs were isolated from adult GSK-3α$^{fl/fl}$ mice and GSK-3α was deleted by adenoviral expression of Cre. After transduction, CFs were treated with TGF-β1 (10 ng/mL) for 10min. Western blotting was carried out; representative Western blot, and quantification of ERK1/2, N=2 for LacZ and Ad-Cre group; N=3 for TGF-β1 treated groups. Data **(7D & 7E)** were analyzed using the Mann-Whitney test and represented as mean ± SEM. Data **(7F & 7G)** were analyzed by Kruskal-Wallis followed by the Dunn test and represented as mean ± SEM.

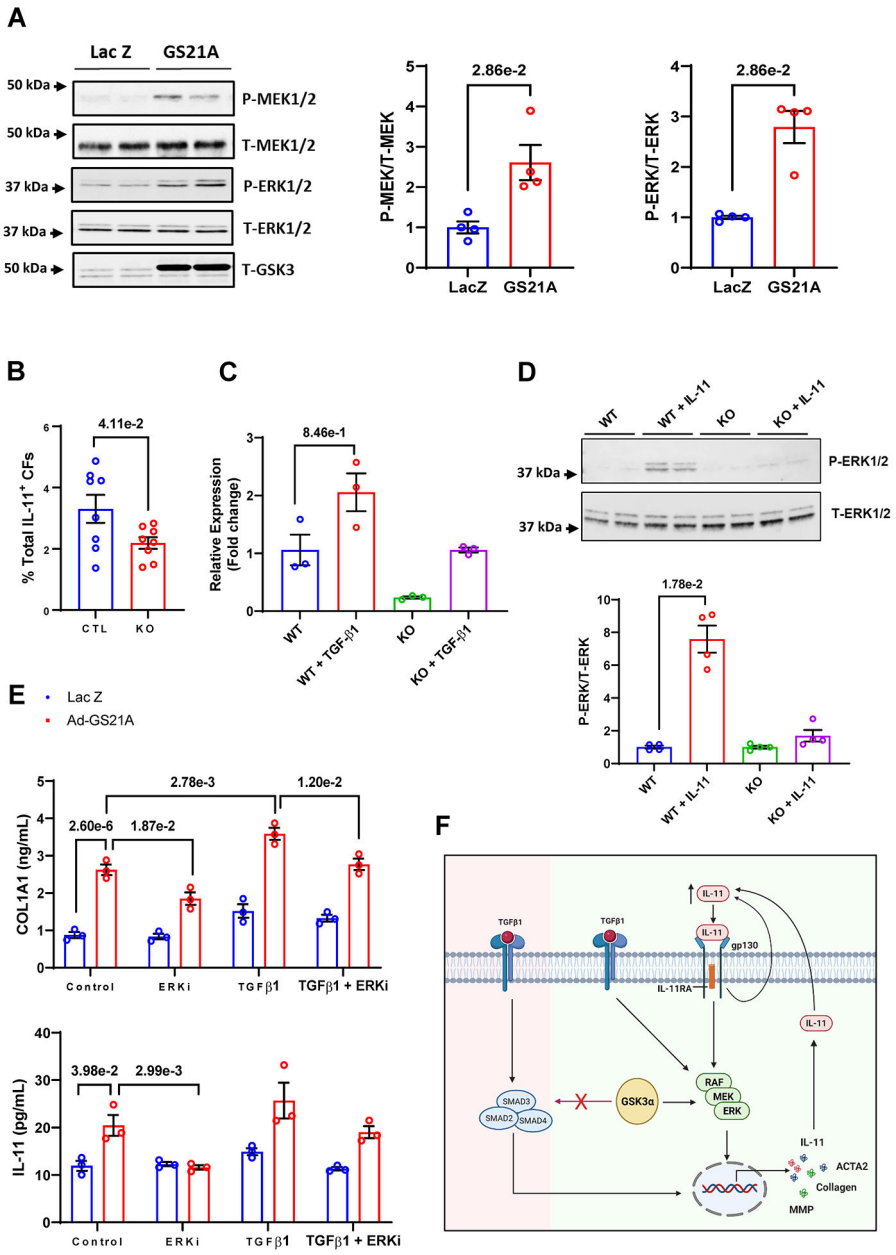

Figure 8: CF-GSK-3α promotes fibrosis through the RAF-MEK-ERK signaling network

(A) For gain-of-function studies, mutant GSK-3α^{S21A} was overexpressed in NRVFs, and protein was extracted after 24h of transfection. Western blotting was performed to examine MEK and ERK levels. N=4 per group. **(B)** At 8 weeks post-TAC, CFs were isolated from CTL and GSK-3α^{FKO} mice. Flow cytometric analysis of IL-11^{+ve} CFs (% total). N=8 per group. **(C)** WT and GSK-3α KO MEFs were treated with TGFβ1 (10 ng/mL, 24h). IL-11 gene expression was analyzed by the qPCR method. The gene expression from each group was normalized to the WT group. N=3 per group. **(D)** For Western blotting, MEFs were treated with IL-11 for 10 min and ERK levels were assessed. Representative blot and quantification. N=4 per group. **(E)** Control and mutant GSK-3α^{S21A} overexpressing NRVFs were treated with ERK inhibitor (U0123, 10μM) for 24h. Culture supernatant was

collected, and ELISA was carried out; quantification of collagen-1 and Il-11. N=3 per group. **(F)** Schematic showing interactions of GSK-3α with IL-11 and ERK signaling pathways in cardiac fibroblast. CF-GSK-3α mediates profibrotic effects through the ERK pathway in the injured heart while classical TGFβ1-SMAD3 signaling remained unaltered. Data **(8A & 8B)** were analyzed using the Mann-Whitney test and represented as mean ± SEM. Data **(8C-8E)** were analyzed by Kruskal-Wallis followed by the Dunn test and represented as mean ± SEM.

Major Resources Table

In order to allow validation and replication of experiments, all essential research materials listed in the Methods should be included in the Major Resources Table below. Authors are encouraged to use public repositories for protocols, data, code, and other materials and provide persistent identifiers and/or links to repositories when available. Authors may add or delete rows as needed.

Animals (in vivo studies)

Species	Vendor or Source	Background Strain	Sex	Persistent ID / URL
GSK-3α $^{fl/fl}$ mice	Dr. Hind Lal (Corresponding author)	C57BL/6J	M, F	
Postn^{MCM} mice	Jackson laboratories, stock #029645	C57BL/6J	M, F	https://www.jax.org/strain/029645
Tcf21^{MCM} mice	Gift from Dr. Michelle D. Tallquist (University of Hawaii, USA)	C57BL/6J	M, F	

Genetically Modified Animals

Species	Vendor or Source	Background Strain	Other Information	Persistent ID / URL
Parent - Male				
Parent - Female				

Antibodies

Target Antigen	Vendor	Catalog #	Working concentration	Persistent ID / URL
p-ERK1/2	Cell Signaling Technology	4370S	1:1000	https://www.cellsignal.com/products/primary-antibodies/phospho-p44-42-mapk-erk1-2-thr202-tyr204-d13-1 type=Products&N=4294956287&Ntt=4370s&fromPage=plp&_requestid=1594512
ERK1/2	Santa Cruz Biotechnology	sc-93	1:1000	https://www.scbt.com/p/erk-1-antibody-c-16
pSMAD3	Abcam	ab52903	1:1000	https://www.abcam.com/smad3-phospho-s423--s425-antibody-ep823y-ab52903.html
Total SMAD3	Abcam	ab40854	1:1000	https://www.abcam.com/smad3-antibody-ep568y-ab40854.html
Lamin A/C	Cell Signaling Technology	2032	1:1000	https://www.cellsignal.com/products/primary-antibodies/lamin-a-c-antibody/2032
GSK-3α/β	Cell Signaling Technology	5676	1:1000	https://www.cellsignal.com/products/primary-antibodies/gsk-3a-b-d75d3-rabbit-mab/5676
GSK-3α	Cell Signaling Technology	4337	1:1000	https://www.cellsignal.com/products/primary-antibodies/gsk-3a-d80e6-rabbit-mab/4337
GAPDH	Fitzgerald	10R-G109a	1:10000	https://fitzgerald-fii.com/gapdh-antibody-10r-g109a.html
β-actin	Santa Cruz Biotechnology	sc-4778	1:10000	https://www.scbt.com/p/beta-actin-antibody-c4
β-tubulin	Proteintech	66240-1-Ig	1:10000	https://www.ptglab.com/products/Tubulin-beta-Antibody-66240-1-Ig.htm
Phospho-MEK1/2	Cell Signaling Technology	9154	1:1000	https://www.cellsignal.com/products/primary-antibodies/phospho-mek1-2-ser217-221-41g9-rabbit-mab/915
Total MEK 1/2	Cell Signaling Technology	9122	1:1000	https://www.cellsignal.com/products/primary-antibodies/mek1-2-antibody/9122

Animals (in vivo studies)

Species	Vendor or Source	Background Strain	Sex	Persistent ID / URL
α- SMA	Sigma-Aldrich	A5228	1:5000	https://www.sigmaaldrich.com/US/en/product/sigma/a5228
p-GSK3β	Cell Signaling Technology	9336	1:1000	https://www.cellsignal.com/products/primary-antibodies/phospho-gsk-3b-ser9-antibody/9336
Total GSK3β	Cell Signaling Technology	9315	1:1000	https://www.cellsignal.com/products/primary-antibodies/gsk-3b-27c10-rabbit-mab/9315
p-Glycogen synthase	Cell Signaling Technology	3891	1:1000	https://www.cellsignal.com/products/primary-antibodies/phospho-glycogen-synthase-ser641-antibody/3891
Total Glycogen synthase	Cell Signaling Technology	3893	1:1000	https://www.cellsignal.com/products/primary-antibodies/glycogen-synthase-antibody/3893
Phospho-p38 MAPK	Cell Signaling Technology	9211	1:1000	https://www.cellsignal.com/products/primary-antibodies/phospho-p38-mapk-thr180-tyr182-antibody/9211
Total p38	Santa Cruz Biotechnology	SC-535	1:1000	https://www.scbt.com/p/p38alpha-antibody-c-20?requestFrom=search
p-ERK1/2	eBioscience	53-9109-42	1:100	https://www.thermofisher.com/antibody/product/Phospho-ERK1-2-Thr202-Tyr204-Antibody-clone-MILAN
MEFSK4 (feeder cell antibody)	Miltenyibiotec	130-120-802	1:100	https://www.miltenyibiotec.com/US-en/products/feeder-cells-antibody-anti-mouse-mef-sk4.html?utm_source=3rd_labome&utm_medium=product_listing&utm_campaign=4_Recombinant_antibodies_for_s ug-in-200-ul
CD31	BD Pharmingen	563356	1:100	https://www.bdbiosciences.com/en-us/products/reagents/flow-cytometry-reagents/research-reagents/single-c cd31.563356
CD45	BD Pharmingen	557659	1:100	https://www.bdbiosciences.com/en-us/products/reagents/flow-cytometry-reagents/research-reagents/single-c cd45.557659
Purified Rat Anti-Mouse CD16/ CD32	BD Pharmingen	553141	1:100	https://www.bdbiosciences.com/en-us/products/reagents/flow-cytometry-reagents/research-reagents/single-c cd16-cd32-mouse-bd-fc-block.553141
IL-11	Santa Cruz Biotechnology	SC-133063 PE	1:100	https://www.scbt.com/p/il-11-antibody-a-9
p-GSK-3α (Ser21)	Cell Signaling Technology	9316	1:100	https://www.cellsignal.com/products/primary-antibodies/phospho-gsk-3a-ser21-36e9-rabbit-mab/9316
α-SMA	Sigma-Aldrich	A5228	1:400	https://www.sigmaaldrich.com/US/en/product/sigma/a5228
α-Actinin	Sigma-Aldrich	SAB4503474	1:200	https://www.sigmaaldrich.com/US/en/product/sigma/sab4503474
Donkey anti-Rabbit, Alexa Fluor 488	Invitrogen	A-21206	1:400	https://www.thermofisher.com/antibody/product/Donkey-anti-Rabbit-IgG-H-L-Highly-Cross-Adsorbed-Seco
Goat anti-Mouse, Alexa Fluor 647	Invitrogen	A-21236	1:400	https://www.thermofisher.com/antibody/product/Goat-anti-Mouse-IgG-H-L-Highly-Cross-Adsorbed-Second
IRDye 680LT Goat anti-Rabbit IgG	LI-COR Biosciences	926-68021	1:3000	https://www.licor.com/bio/reagents/irdye-680lt-goat-anti-rabbit-igg-secondary-antibody
IRDye® 800CW Goat anti-	LI-COR Biosciences	925-32210	1:3000	https://www.licor.com/bio/reagents/irdye-800cw-goat-anti-mouse-igg-secondary-antibody

Animals (in vivo studies)

Species	Vendor or Source	Background Strain	Sex	Persistent ID / URL
Mouse IgG				

DNA/cDNA Clones

Clone Name	Sequence	Source / Repository (Gift from following Scientists)	Persistent ID / URL
Ad-LacZ	-	Dr. David E. Dostal (Texas A&M University)	
Ad-GSK3α-S21A	-	Dr. James Woodgett (Lunenfeld-Tanenbaum Research Institute, Canada)	
Ad-GSK3α	-	Dr. Junichi Sadoshima(Rutgers New Jersey Medical School)	

Cultured Cells

Name	Vendor or Source	Sex (F, M, or unknown)	Persistent ID / URL
Mouse embryonic fibroblasts	Gift from Dr. James Woodgett (Lunenfeld-Tanenbaum Research Institute, Canada)	Unknown	
Neonatal rat ventricular fibroblasts	2-3 day old rat pups	M, F	
Adult mouse cardiac fibroblasts	3 montds old mice	M, F	

Data & Code Availability

Description	Source / Repository	Persistent ID / URL

Other

Primers used for qPCR	Vendor	Assay ID	Catalog #
COL1A1	Applied Biosystems	Mm00801666_g1	4331182
COL3A1	Applied Biosystems	Mm00802296_g1	4331182
ANP	Applied Biosystems	Mm01255747_g1	4331182
BNP	Applied Biosystems	Mm01255770_g1	4331182
Fibronectin −1	Applied Biosystems	Mm01256744_m1	4331182
IL-11	Applied Biosystems	Mm00434162_m1	4331182
Eukaryotic 18S rRNA Endogenous Control	Applied Biosystems	-	4319413E

Other

Description	Vendor	Catalog #
Hematoxylin-Eosin	Sigma-Aldrich	HT1079
Trichrome Stain (Masson) Kit	Sigma-Aldrich	HT15
RNeasy Mini Kit	Qiagen	74104
iScript cDNA synthesis kit	Bio-rad	170-8891
TaqMan Gene Expression Master Mix	Applied Biosystems	4369016
ProLong Gold antifade reagent with DAPI	Invitrogen	P36941

Other

Description	Vendor	Catalog #
Antigen Unmasking Solution	Vector Lab Inc	H-3300
cell lysis buffer	Cell signaling Technology	9803S
Protease Inhibitor Cocktail	Sigma-Aldrich	P8340
Phosphatase Inhibitor Cocktail	Sigma-Aldrich	P0044
NE-PER Reagent	Pierce	78833
Bio-Rad Protein Assay Dye	Bio-rad	5000006
Odyssey blocking buffer	LI-COR Biosciences	927-40000
Immobilon-P PVDF membrane	EMD Millipore	IPVH00010
TGFβ1	Sigma-Aldrich	T7039
recombinant mouse IL-11	R&D Systems	418-ML-005
PureCol® 3 mg/ml, Type I collagen stock solution	Advanced Biomatrix	5005
BrdU labeling and detection kit	Roche	11296736001
BrdU	Sigma-Aldrich	B5002
U0126	LC Laboratories	U-6770
Rat Collagen I alpha 1 ELISA Kit (Colorimetric)	Novus biologicals	NBP2-75840
Rat IL-11 ELISA Kit (Colorimetric)	Novus biologicals	NBP3-06795
MidiMACS™ Separator and Starting Kits	Miltenyi Biotec	130-042-301
CD31 MicroBeads, mouse	Miltenyi Biotec	130-097-418
CD45 MicroBeads, mouse	Miltenyi Biotec	130-052-301